Feasibility study of a nuclear exciton laser

Nicolai ten Brinke and Ralf Schützhold*
Fakultät für Physik, Universität Duisburg-Essen, Lotharstrasse 1, D-47057 Duisburg, Germany

Dietrich Habs
Fakultät für Physik, Ludwig-Maximilians-Universität München, Am Coulombwall 1, D-85748 Garching, Germany
(Received 7 August 2012; revised manuscript received 28 March 2013; published 9 May 2013)

Nuclear excitons known from Mössbauer spectroscopy describe coherent excitations of a large number of nuclei—analogous to Dicke states (or Dicke super-radiance) in quantum optics. In this paper, we study the possibility of constructing a laser based on these coherent excitations. In contrast to the free-electron laser (in its usual design), such a device would be based on stimulated emission and thus might offer certain advantages, e.g., regarding energy-momentum accuracy. Unfortunately, inserting realistic parameters, the window of operability is probably not open (yet) to present-day technology; but our design should be feasible in the UV regime, for example.

DOI: 10.1103/PhysRevA.87.053814 PACS number(s): 42.55.Vc, 42.55.Ah, 42.50.Gy, 33.25.+k

I. INTRODUCTION

The invention of the laser led to a giant leap in the field of classical and quantum optics. This light source offers unprecedented possibilities regarding features such as coherence, intensity, and brilliance. Unfortunately, however, it is not easy to transfer this successful concept beyond the optical or near-optical regime, see [1,2]. Free-electron lasers, for example, work at much higher energies; but their principle of operation (in their usual design) is more similar to classical emission than to stimulated emission. As a result, their properties (e.g., regarding coherence) are not quite comparable to optical lasers.

There is another phenomenon in this energy range on the order of keV in which coherence plays a crucial role: nuclear excitons known from Mössbauer spectroscopy [3,4]. These coherent excitations of a large number of nuclei [5–7] are analogous to Dicke states [8] (also known as Dicke super-radiance [9–11]) in quantum optics. The coherence results in constructive interference of the emission amplitudes from many nuclei [12] and is facilitated by the fact that the photon recoil is absorbed by the whole lattice [3,4] instead of the individual nuclei (which would destroy the coherence). For example, the coherent nature of the propagation of nuclear excitons through resonant media, showing quantum beats, was observed in Refs. [13,14]. Other cooperative effects of coherently excited nuclei have been studied, such as the collective Lamb shift [15], coherent control of nuclear x-ray pumping [16], and electromagnetically induced transparency [17].

In the following, we study the possibility of constructing a laser-type device employing these nuclear excitons, which is based on stimulated emission [18]. Such a device could combine the advantages of the free-electron laser with the coherence and brilliance of nuclear excitons. Of course, this is not the first proposal along these lines. The idea of constructing a laser-type device employing these nuclear excitons was brought up already about half a century ago; see, e.g., [19–21]. Since then, a vast amount of research has been conducted on the topic, following different approaches to pumping. For example, there have been proposals to pump the nuclei directly to the laser level via radiation or bursts of particles [22–24], concepts which employ nuclear isomers [24–26], and approaches which try to circumvent the requirement of creating a population inversion [20,27,28]. The major problem in all these approaches is that the required high intensity for pumping is either not achievable with available sources or so large that it destroys the gain medium. This problem is often referred to as the so-called graser dilemma, see [1].

In our setup, we consider direct pumping via a coherent radiation pulse, which can be very short and thus very broad in frequency—the brilliance of the emitted beam is caused by the nuclear excitons. Furthermore, the radiation which stimulates the emission is also created by the collective decay of a large number of "seed" nuclei. Both features can help us to reduce the aforementioned graser dilemma, but—as we shall see in Sec. VI below—we cannot completely overcome this obstacle (at least not for x rays).

II. HAMILTONIAN

First, we describe a single nucleus as a two-level system with transition frequency ω interacting resonantly with a single-mode field. In a rotating-wave and dipole approximation, the Hamiltonian can then be cast into the standard form ($\hbar = c = \varepsilon_0 = 1$)

$$\hat{H}_{\text{single}} = (g\hat{a}\sigma_\ell^+ e^{i\boldsymbol{\kappa}\cdot\boldsymbol{r}_\ell} + \text{H.c.}) + \frac{\omega}{2}\left(\sigma_\ell^z + 1\right) + \omega\hat{a}^\dagger\hat{a}. \qquad (1)$$

As usual, the ladder operators $\sigma_\ell^\pm = (\sigma_\ell^x \pm i\sigma_\ell^y)/2$ and the Pauli matrix σ_ℓ^z describe the two-level system. The first term governs the interaction (with coupling constant g) with the electromagnetic field and thus contains photonic annihilation and creation operators $\hat{a}$,$\hat{a}^\dagger$ and phase factors $e^{i\boldsymbol{\kappa}\cdot\boldsymbol{r}_\ell}$ depending on the location of the nucleus, $\boldsymbol{r}_\ell$, and the wave number $\boldsymbol{k} = \boldsymbol{\kappa}$ of the photon mode with $|\boldsymbol{\kappa}| = \omega$. The second and third terms account for the energy stored in the two-level nucleus and in the single-mode field, respectively. When dealing with many $S \gg 1$ two-level nuclei instead of one, we can sum up the

*ralf.schuetzhold@uni-due.de

individual-nucleus Hamiltonians and arrive at

$$\hat{H} = (g\hat{a}\hat{\Sigma}^{+} + \text{H.c.}) + \omega\left(\hat{\Sigma}^{z} + \frac{S}{2}\right) + \omega\hat{a}^{\dagger}\hat{a}, \tag{2}$$

where quasispin S operators have been introduced

$$\hat{\Sigma}^{\pm} = \sum_{\ell=1}^{S} \sigma_{\ell}^{\pm} \exp\{\pm i\boldsymbol{\kappa}\cdot\boldsymbol{r}_{\ell}\}, \quad \hat{\Sigma}^{z} = \frac{1}{2}\sum_{\ell=1}^{S}\sigma_{\ell}^{z}. \tag{3}$$

In the interaction picture, the perturbation Hamiltonian, originating from the first term in Eq. (2), reads

$$\hat{V} = g\hat{a}\hat{\Sigma}^{+} + \text{H.c.} \tag{4}$$

The quasispin S operators $\hat{\Sigma}^{\pm} = \hat{\Sigma}^{x} \pm i\hat{\Sigma}^{y}$ and $\hat{\Sigma}^{z}$ generate an SU(2) algebra [29]. Thus, the transition matrix elements for collective transitions depend not only on the number of nuclei involved but also on the number of excitations s, i.e.,

$$\begin{aligned} \hat{\Sigma}^{+}|s\rangle &= \sqrt{(S-s)(s+1)}\,|s+1\rangle, \\ \hat{\Sigma}^{-}|s\rangle &= \sqrt{(S-s+1)s}\,|s-1\rangle, \end{aligned} \tag{5}$$

where $|s\rangle \propto (\hat{\Sigma}^{+})^{s}|0\rangle$ denotes a coherent state with s excitons, often referred to as Dicke states [8].

III. COHERENT EMISSION

In contrast to the spontaneous decay of a single excited nucleus, where the resulting photon can be emitted in all directions, exciton states as in Eq. (5) predominantly emit photons in the forward direction $\boldsymbol{\kappa}$. Only in this case, all the phases $e^{i\boldsymbol{\kappa}\cdot\boldsymbol{r}_{\ell}}$ add up coherently (we assume random locations $\boldsymbol{r}_{\ell}$), see Fig. 1. We will now investigate spontaneous and stimulated emissions from an ensemble of S coherently excited nuclei in more detail. In the following, we consider the thin foil limit; i.e., we assume that a photon, once emitted, leaves the foil without further interaction.

A. Spontaneous emission

We start with the case of collective spontaneous emission (also know as the Dicke super-radiance [9–11]) from a coherent state $|s\rangle$. First of all, as the S nuclei are not enclosed by a resonator or a cavity in our setup, we have to consider all $\boldsymbol{k}$ modes. Thus, the Hamiltonian (4) changes into

$$\hat{V}_{\text{sp}}(\tau) = \int d^{3}k\; g_{\boldsymbol{k}}\hat{a}_{\boldsymbol{k}}\, e^{-i(\omega_{\boldsymbol{k}}-\omega)\tau}\hat{\Sigma}^{+}(\boldsymbol{k}) + \text{H.c.}, \tag{6}$$

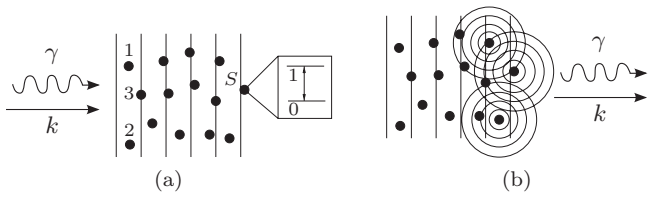

FIG. 1. Sketch of the coherent properties of nuclear excitons. An incident photon with wave vector $\boldsymbol{k}$ is absorbed (a) by an ensemble of $S \gg 1$ nuclei (two-level systems) and thus generates a Dicke state $|s=1\rangle$. Then the decay amplitudes of all these nuclei add up coherently in the forward direction such that absorption is followed by collective spontaneous emission into the same direction (b).

where $\hat{a}_{\boldsymbol{k}}$ is the photonic annihilation operator for the mode $\boldsymbol{k}$ with frequency $\omega_{\boldsymbol{k}}$ and $g_{\boldsymbol{k}}$ the associated coupling strength. Note that we neglect polarization effects, i.e., we assume that the polarization vectors are directed along the same axis as the dipole moments of the absorbing nuclei. Furthermore, $\hat{\Sigma}^{+}(\boldsymbol{k})$ denotes the quasispin S operators with the wave number $\boldsymbol{k}$ instead of $\boldsymbol{\kappa}$. However, when $\boldsymbol{k}$ is not close to $\boldsymbol{\kappa}$, the phase factors of $\hat{\Sigma}^{\pm}(\boldsymbol{k})$ and $|s\rangle$ do not match, and the transition is not coherent, i.e., not enhanced by a factor S according to Eq. (5), and can thus be neglected. Note that this is the reason why collectively emitted photons are directed along (almost) the same axis as previously absorbed photons [9–11], see also Fig. 1. For simplicity, the quasispin S operators are therefore approximated by introducing a cutoff function $g(\boldsymbol{\kappa}-\boldsymbol{k})$ that is only nonzero for small deviations $\boldsymbol{\kappa}-\boldsymbol{k}$ of the supported direction $\boldsymbol{\kappa}$, i.e., $\hat{\Sigma}^{\pm}(\boldsymbol{k}) \approx g(\boldsymbol{\kappa}-\boldsymbol{k})\,\hat{\Sigma}^{\pm}$.

For large S, we may approximate the quasispin S operators classically, i.e., $\hat{\Sigma}^{-} \approx \Sigma^{-} = \sqrt{(S-s+1)s}$, and hence the effect of the Hamiltonian (6) acting on the vacuum state can be expressed by a coherent state

$$\hat{U}_{\text{sp}}(t)\,|0\rangle \approx \exp\left(\int d^{3}k\,\alpha_{\boldsymbol{k}}\hat{a}_{\boldsymbol{k}}^{\dagger} - \text{H.c.}\right)|0\rangle, \tag{7}$$

with the amplitudes

$$i\alpha_{\boldsymbol{k}} = g_{\boldsymbol{k}}^{*}g(\boldsymbol{\kappa}-\boldsymbol{k})\sqrt{(S-s+1)\,s}\int_{0}^{t} d\tau\, e^{i(\omega_{\boldsymbol{k}}-\omega)\tau}. \tag{8}$$

The number of emitted photons per mode is given by $|\alpha_{\boldsymbol{k}}|^{2}$ and the total photon number grows linearly with t

$$\mathcal{N}_{\gamma} = \int d^{3}k\,|\alpha_{\boldsymbol{k}}|^{2} \approx 2\pi^{2}(S-s+1)\,s|g_{\boldsymbol{\kappa}}|^{2}\frac{t}{L_{\perp}^{2}}, \tag{9}$$

where $L_{\perp}^{2}$ denotes the transversal cross-section area of the ensemble, which determines the transverse area in $\boldsymbol{k}$ space where $g(\boldsymbol{\kappa}-\boldsymbol{k})$ is nonzero. In addition to this spatial resonance condition, the temporal resonance was incorporated via approximating the squared time integral by t^{2} for $|\omega_{\boldsymbol{k}}-\omega| < 1/t$ and zero otherwise.

Strictly speaking, this relation is only valid for a fixed number of excitations s, i.e., the time dependence of $s(t)$ due to the emission of photons (energy conservation) is neglected. Assuming that this time dependence $s(t)$ is slow compared to ω (i.e., that the coupling strength is small enough), we may take it into account approximately by defining the instantaneous spontaneous emission rate

$$\Gamma_{\text{sp}}(t) = \frac{d\mathcal{N}_{\gamma}}{dt} = \gamma[S-s(t)+1]s(t), \tag{10}$$

with the abbreviation $\gamma = 2\pi^{2}|g_{\boldsymbol{\kappa}}|^{2}/L_{\perp}^{2}$. The change of $s(t)$ in the time interval dt is then governed by $\Gamma_{\text{sp}}(t)$

$$\frac{ds(t)}{dt} = -\Gamma_{\text{sp}}(t) = -\gamma[S-s(t)+1]s(t). \tag{11}$$

For the initial condition $s(0) = S/2$ (see below), the solution for $S \gg 1$ is given by

$$s(t) = \frac{S}{1+e^{\gamma St}}. \tag{12}$$

This yields the intensity due to spontaneous emission

$$I_{\rm sp}(t) = -\frac{dE}{dt}\frac{1}{L_\perp^2} = -\frac{ds(t)}{dt}\frac{\omega}{L_\perp^2} = \frac{1}{4}\gamma S^2 \mathrm{sech}^2(\gamma S t/2)\,\frac{\omega}{L_\perp^2}, \tag{13}$$

where $L_\perp^2$ is the cross-section area of the emitted beam, see also [30]. The time dependence in the sech function can be used to define an effective time constant via

$$\tau_{\rm sp} = \frac{4}{\gamma S}, \tag{14}$$

after which $I_{\rm sp}(t)$ has dropped to 7% of its initial value. Let us now briefly compare this time scale $\tau_{\rm sp}$ for the coherent spontaneous emission process with the time scale in the incoherent case. For incoherent emission from s excited nuclei, we can regard each nucleus independently. According to standard Weisskopf-Wigner theory [31], the lifetime of an excited nucleus is given by

$$\tau_{\rm single} = \frac{1}{\Gamma_{\rm single}} = \frac{1}{8\pi^2}\frac{1}{|g_\kappa|^2\omega^2}. \tag{15}$$

Comparing the two time scales in Eqs. (14) and (15)

$$\frac{\tau_{\rm sp}}{\tau_{\rm single}} = 64\pi^2\frac{L_\perp^2}{\lambda^2}\frac{1}{S}, \tag{16}$$

we find that for large S, the coherent spontaneous emission process is much faster than the incoherent process (see also [32]). Taking for example $S = 10^{10}$ ^{57}Fe nuclei with resonance at $\Delta E_\gamma = 14.4$ keV, lifetime $\tau_{\rm single} = 141$ ns and $L_\perp = 0.1$ μm, the quotient evaluates to $\tau_{\rm sp}/\tau_{\rm single} \approx 0.09$, i.e., the coherent emission runs over ten times faster than the incoherent emission. However, as the foil would then be about $d_{\rm Fe} = 12$ μm thick, the thin-foil limit is not a good approximation anymore. More realistic experimental values are discussed in Sec. VI below. Note that there are also competing processes, such as decay via electron conversion; but they are incoherent and thus can be suppressed for large S, i.e., small $\tau_{\rm sp}$.

B. Stimulated emission

To study stimulated emission from a coherently excited S-nuclei ensemble, we regard the incoming field $A_{\rm in}(t) = \sqrt{I_{\rm in}(t)}/\omega$ classically. That is, we use the Hamiltonian (4), but replace $g\hat{a}$ by $\tilde{g}A_{\rm in}(t)$. For simplicity, we assume the transition matrix element $\tilde{g}$ of the nucleus to be real

$$\hat{V}_{\rm st} = \tilde{g}A_{\rm in}(t)(\hat{\Sigma}^+ + \hat{\Sigma}^-) = 2\tilde{g}A_{\rm in}(t)\hat{\Sigma}^x. \tag{17}$$

Applying the Heisenberg picture and employing the properties of the SU(2) algebra yields

$$\hat{U}_{\rm st}^\dagger(t)\hat{\Sigma}^z\hat{U}_{\rm st}(t) = \cos\left(2\tilde{g}\int_0^t d\tau\, A_{\rm in}(\tau)\right)\hat{\Sigma}^z + \sin\left(2\tilde{g}\int_0^t d\tau\, A_{\rm in}(\tau)\right)\hat{\Sigma}^y. \tag{18}$$

As envisaged for the laser application (see below), we choose $s(0) = S$ here, that is, all S nuclei are in the coherently excited state. The time-dependent number of excitations is given by $\langle S|\hat{U}_{\rm st}^\dagger(t)\hat{\Sigma}^z\hat{U}_{\rm st} + S/2|S\rangle$ and thus the energy stored in the S nuclei at time t is

$$E(t) = \frac{S\omega}{2}\left[\cos\left(2\tilde{g}\int_0^t d\tau\, A_{\rm in}(\tau)\right) + 1\right]. \tag{19}$$

This yields the emitted intensity $I_{\rm st}(t)$ stimulated by the incoming intensity $I_{\rm in}(t)$

$$I_{\rm st}(t) = \frac{\tilde{g}S}{L_\perp^2}\sin\left(\frac{2\tilde{g}}{\omega}\int_0^t d\tau\,\sqrt{I_{\rm in}(\tau)}\right)\sqrt{I_{\rm in}(t)}, \tag{20}$$

where we have assumed that both beams have the same cross-section area $L_\perp^2$.

We define the time scale of the stimulated emission as the time $\tau_{\rm st}$, after which all the energy initially stored in the S nuclei has been emitted, i.e.,

$$\int_0^{\tau_{\rm st}} d\tau\,\sqrt{I_{\rm in}(\tau)} = \frac{\pi\omega}{2\tilde{g}}. \tag{21}$$

Now let us imagine that we have two separate ensembles (e.g., foils) of coherently excited nuclei, such that the first foil spontaneously emits the intensity $I_{\rm in}(t)$ as in Eq. (13) which causes stimulated emission according to Eq. (20) in the second foil. In this case, we can insert $I_{\rm in}(t) = I_{\rm sp}(t)$, and Eq. (21) can be solved for $\tau_{\rm st}$:

$$\tau_{\rm st} = \frac{4}{\gamma S}\,\mathrm{ArTanh}\left[\mathrm{Tan}\left(\frac{1}{8}\sqrt{\frac{\pi}{2}}\right)\right] \approx 0.16\times\tau_{\rm sp}. \tag{22}$$

Since both foils contain the same nuclei (with the same coupling strengths), the time scale for the stimulated emission of the second foil, $\tau_{\rm st}$, is completely determined by the time scale of the spontaneous emission process of the first foil, $\tau_{\rm sp}$.

IV. PUMPING

After having discussed coherent spontaneous emission as well as coherent stimulated emission, let us investigate the pumping process for a single foil of S nuclei, which are initially in the state $s = 0$, i.e., $\langle 0|\hat{\Sigma}^z|0\rangle = -S/2$. Note that it is very easy to over- or under-estimate the efficiency of the pumping process by using too simplified pictures. On the one hand, one might expect that the number of excitons in the foil grows linearly with the number of photons incident and thus linearly with the interaction time t. However, this is only true for pumping with incoherent light (for further details, see the Appendix), but not for coherent pumping, which is the case considered here. On the other hand, since the transition matrix elements in Eq. (5) scale with $\sqrt{s}$ and thus the effective linewidth increases with s, one might expect a behavior like $\dot{s} \propto s$, which would imply an exponential growth $s(t) \propto e^{\kappa t}$, at least for small $s \ll S$. This picture is also wrong, since—in view of the unitarity of the time evolution—not just the absorption rate but also the emission rate increases with s. Thus, the correct answer is that $s(t)$ grows quadratically $s(t) \propto t^2$ for small s, i.e., somewhere in between linear and exponential.

To show this, let us consider pumping with one coherent pump pulse $A_{\rm pump}(t)$ for the whole interaction time. We can employ the Hamiltonian (17) again with the sole difference that the incoming field $A_{\rm in}(t)$ is now given by the pump field

$A_{\rm in}(t) = A_{\rm pump}(t)$. Thus, Eq. (18) again holds, and the exciton number is given by

$$s(t) = \frac{S}{2}\left[1 - \cos\left(2\tilde{g}\int_0^t d\tau\, A_{\rm pump}(\tau)\right)\right] = S\tilde{g}^2\left(\int_0^t d\tau\, A_{\rm pump}(\tau)\right)^2 + O(\tilde{g}^4 t^4), \quad (23)$$

i.e., the exciton number grows quadratically for small t (for an alternative approach, see the Appendix). We moreover find that a full cycle (i.e., a sign flip of $\hat{\Sigma}^z \to -\hat{\Sigma}^z$) occurs after the pump time $\tau_{\rm pump}$ where

$$\int_0^{\tau_{\rm pump}} d\tau\, A_{\rm pump}(\tau) = \frac{\pi}{2\tilde{g}}. \quad (24)$$

The simplest example would be a constant pump pulse $A_{\rm pump} = A_0$ with $\tau_{\rm pump} = \pi/(2\tilde{g}A_0)$. To see if such a pump field is feasible in general, we calculate a rough estimate of the required intensity of the pump field. For simplicity, we assume that the intensity is constant over the pulse, i.e., $A_{\rm pump}(t) = \sqrt{I_{\rm pump}}/\omega$. Then we find $I_{\rm pump} = \pi^2\omega^2/(4\tilde{g}^2\tau_{\rm pump}^2)$. Now $\tilde{g}$ can be expressed in terms of the (single-nucleus) decay rate $\Gamma_{\rm single}$ and the frequency ω of the considered nuclear excitation (see the Appendix). Moreover, if we replace the coherent pulse length $\tau_{\rm pump} = \mathfrak{N}\lambda = 2\pi\mathfrak{N}/\omega$ by the number $\mathfrak{N}$ of (coherent) wave cycles, we find

$$I_{\rm pump} = \frac{1}{32\pi\mathfrak{N}^2}\frac{\omega^5}{\Gamma_{\rm single}}. \quad (25)$$

Thus, nuclear resonances with low energies ω but high decay rates $\Gamma_{\rm single}$ require low pump intensities. Concrete examples will be discussed at the end of this article.

V. LASER

Now we have gathered all the tools required to understand the setup of the proposed nuclear exciton laser. The envisaged setup consists of a series of $N \gg 1$ foils $n = 1,2,\ldots,N$, each foil containing S_n nuclei (two-level systems) with a nuclear resonance at frequency ω. At the beginning, we assume that all $n = 1,2,\ldots,N$ foils are in the ground state, corresponding to a quasispin $\Sigma_n^z = -S_n/2$, see Fig. 2(a).

To prepare the emission of a laser pulse, the foils need to be pumped to suitable coherent states. For simplicity, we envisage the whole pumping process to be achieved by a single coherent pump pulse, which goes through all the foils one after another and is only weakly changed by absorption. Since the pump pulse consists of many (e.g., about 10^{12}) photons in a coherent state, it can be approximately regarded as a classical field. Thus, the pump pulse basically does not generate any entanglement between the foils and hence they can be treated independently. Note that this would change if we were to pump with single photons—in this case, we would create an excitonic state across all foils, i.e., with interfoil entanglement.

Let us distinguish between the first foil and all later foils $n = 2,\ldots,N$. While the latter all should be pumped to the maximum of $\Sigma_n^z = S_n/2$, i.e., $s_n = S_n$, the first foil should only be pumped such that half of the nuclei are in the excited state, i.e., $\Sigma_1^z = 0$ and $s_1 = S_1/2$.

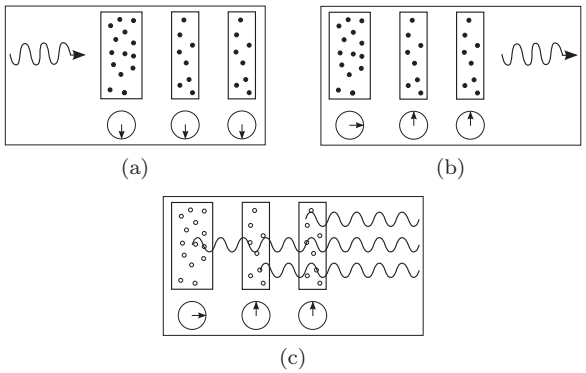

FIG. 2. Sketch of the operation sequence of the proposed nuclear exciton laser. Initially, all foils (here $N = 3$) are in the ground state $\Sigma_n^z = -S_n/2$ (a). The pump pulse then rotates the quasispin of the first foil to $\Sigma_1^z = 0$ and the quasispin of all subsequent foils to $\Sigma_n^z = +S_n/2$ (b). Then, the "half-filled" first foil spontaneously emits a pulse $I_{\rm sp}(t)$, which stimulates emission at foils 2 and 3, leading to an enhanced overall intensity $I_{\rm total}^{(3)}(t)$ (c).

The pump pulse should satisfy Eq. (24) in order to rotate the quasispin Σ_n^z of each foil from $\Sigma_n^z = -S_n/2$ to $\Sigma_n^z = +S_n/2$. Additional measures need to be taken to ensure that the first foil is only pumped to $s_1 = S_1/2$. One option could be to have a different kind of nuclei in the first foil, which have the same resonance frequency as those in the other foils, while the coupling strengths differ by a factor of 2 (approximately). For nuclear transitions this requirement is probably hard to achieve. However, for optical transitions, which we will also discuss in Sec. VI, this method may be feasible. Another option could be to switch the first foil mechanically or magnetically [33–37] during the pumping process. For the case of magnetic switching, the foils could be made of $^{57}FeBO_3$ crystals as in Refs. [33,36], for example. After half of the nuclei in the first foil have been excited by the pump pulse, the direction of the crystal magnetization would be changed abruptly via an external magnetic field. After the pump pulse has completely passed the first foil, the crystal magnetization would be switched back. However, it is not clear if the magnetic switching could be conducted sufficiently quickly, because the pump pulse is very short (in the range of ps). Thus it may be preferable to switch the first foil mechanically [34]. To destroy the (spatial) phase coherence between the excitonic state with $s_1 = S_1/2$ and the incoming pump pulse it suffices that the foil is rotated such that an atom sitting at the border of the foil is moved about half a wavelength $\lambda/2$. This can be done by tilting or rotating the foil after half of the nuclei have been excited. For the parameters discussed in Sec. VI below, this would correspond to a moderate velocity of a few hundred meters per second and an angular velocity of order 10^{10} Hz, i.e., in the hypersound regime.

When the setup is prepared as shown in Fig. 2(b), the emission process automatically starts, as the first foil immediately begins with the spontaneous emission discussed above, Eq. (13). The idea is that due to the "half-filled" coherent state $\Sigma_1^z = 0$, the emission process of the first foil happens much faster than the spontaneous emission of the subsequent foils. Taking, e.g., the second foil ($s_2 = S_2$), the time scale for the

emission of a single photon would be $1/\Gamma_{sp} = 1/(\gamma S_2)$. For the first foil, the time scale for the whole emission process (of nearly all photons, not only one) is given by $\tau_{sp} = 4/(\gamma S_1)$. So by choosing $S_1 \gg S_2$, e.g., by making the first foil ten times thicker than the subsequent foils, it is ensured that the second foil is still in the state $\Sigma_2^z = S_2/2$, when the intensity emitted from the first foil is incident.

Stimulated emission then occurs at the second foil according to Eq. (20) and the second foil has emitted all its energy after $\tau_{st} \approx 0.16 \times \tau_{sp}$, i.e., before the stimulating pulse coming from the first foil declines. After the second foil, the overall intensity thus adds up to $I^{(2)}_{total}(t) = I_{sp}(t) + I^{(2)}_{st}(t)$. This overall intensity then causes stimulated emission at the third foil, resulting in an even bigger intensity $I^{(3)}_{total}(t) = I^{(2)}_{total}(t) + I^{(3)}_{st}(t)$, etc. In this way, the intensity of the light pulse grows stepwise with each passed foil.

Numerical analysis has been done for the case of $N = 50$ foils. Iteratively, $I^{(n)}_{st}(t)$ was calculated from $I^{(n-1)}_{total}(t)$, where $I^{(n)}_{total}(t) = I^{(n-1)}_{total}(t) + I^{(n)}_{st}(t)$, starting with $I^{(1)}_{total}(t) = I_{sp}(t)$. It was assumed that the first foil consists of $S_1 = 10^{10}$ ^{57}Fe nuclei (with $\Delta E_\gamma = 14.4$ keV and $\tau = 141$ ns) while all other foils are ten times thinner, i.e., $S_n = 10^9$. Transversal dimensions of the foils and the laser beam are chosen as $L_\perp^2 = (0.1\ \mu\text{m})^2$.

Note that the useful part of the laser pulse $I^{(n)}_{total}(t)$ is determined by the time after which the last foil has emitted all its excitations, $\tau^{(n)}_{st}$, because afterward reabsorption takes place. (The undesired effect of reabsorption of parts of the laser pulse in a *succession of thin foils* can be regarded in analogy to dynamic beats occurring in *one thick foil*.) This time $\tau^{(n)}_{st}$ becomes shorter with rising n, as the intensity which causes the stimulated emission grows with n. As a result, the average intensity of the useful part of the laser pulse,

$$\overline{I^{(n)}_{total}} = \frac{1}{\tau^{(n)}_{st}} \int_0^{\tau^{(n)}_{st}} d\tau\ I^{(n)}_{total}(\tau), \tag{26}$$

increases with a power law. In the concrete example given above, $\overline{I^{(n)}_{total}}$ grows roughly $\propto n^{3/2}$, see Fig. 3.

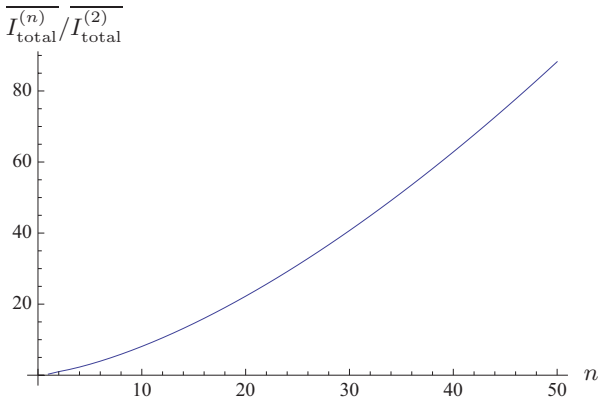

FIG. 3. (Color online) Average intensity $\overline{I^{(n)}_{total}}$ over number of foils n from numerical analysis. In this example, $\overline{I^{(n)}_{total}}$ roughly increases as a power law $\propto n^{3/2}$.

VI. CONCLUSIONS

In summary, we described a proposal for a laser in the keV regime which is based on stimulated emission and works with nuclear excitons. The pumping could be achieved with a free-electron laser, for example. Note that the pump pulse A_{pump} and the generated laser pulse A_{laser} both correspond to a 180° rotation of the last foil according to Eq. (18) and thus are related via

$$\int_0^{\tau_{pump}} d\tau\ A_{pump}(\tau) = \int_0^{\tau^{(N)}_{st}} d\tau\ A_{laser}(\tau) = \frac{\pi}{2\tilde{g}}. \tag{27}$$

However, the intensity of the pump pulse $\propto |A^2_{pump}|$ is much larger than that of the laser pulse $\propto |A^2_{laser}|$. On the other hand, the duration $\tau^{(N)}_{st}$ of the laser pulse is much larger and thus its frequency accuracy is much higher (see also [38] for a different approach). This could be important for spectroscopy, etc.

Let us discuss some example data for the required intensity of the pump pulse. First, we consider ^{57}Fe nuclei with a resonance at $\Delta E_\gamma = 14.4$ keV with a mean lifetime of $\tau = 141$ ns. If we assume that the pump pulse consists of $\mathfrak{N} = 10^6$ coherent wave trains, we would need a pump intensity of $I_{pump} \approx 8.3 \times 10^{20}$ W/cm^2 according to Eq. (25). (Comparable or even higher intensities have already been considered in, e.g., [39–41].) This is probably beyond the capabilities of present free-electron lasers; see, e.g., [42]. However, future light sources such as seeded free-electron lasers should achieve improved coherence times and higher intensities (especially after focusing with x-ray lenses). In addition, a foil consisting of $S_1 = 10^{10}$ ^{57}Fe atoms and transversal dimensions of $L_\perp = 0.1\ \mu$m is about $d_{Fe} = 12\ \mu$m thick and thus we would need to take dynamical beats [14,43] into account.

On the other hand, when considering other nuclear resonances beyond the well-known ^{57}Fe example, we find that the requirements are somewhat easier to fulfill. For example, considering the ^{201}Hg resonance at $\Delta E_\gamma = 1.6$ keV with $\tau = 81$ ns and again assuming $\mathfrak{N} = 10^6$ coherent wave trains, we would "only" need a pump intensity of $I_{pump} \approx 8.0 \times 10^{15}$ W/cm^2 according to Eq. (25). This pump intensity may possibly be reached by the European X-Ray Laser Project (XFEL) using a self-seeding scheme [44]. Furthermore, the thin foil limit is legitimate here, since the ^{201}Hg foils can be made much thinner than the ^{57}Fe foils. According to Eq. (16), we can for example choose $L_\perp = 0.5\ \mu$m and $d_{Hg} = 1\ \mu$m to store $S_1 = 10^{10}$ nuclei.

Unfortunately, this intensity is probably still too large for another reason: After inserting typical values for the absorption cross section of 1.6 keV photons in metals (or other solid materials), we find that the pump beam deposits enough energy in the foil to evaporate it. Even though the thermalization dynamics following the illumination with such a 8.0×10^{15} W/cm^2 beam of 1.6 keV photons is not well studied yet, one would expect that the foil starts to disintegrate after a few picoseconds [45] and hence does not survive long enough for our purposes.

In summary, the major difficulty of our setup is that it requires extremely large pump intensities. As we may infer from Eq. (25), the pump intensity scales with the fifth power of the transition energy ω. Thus, our scheme should be much easier to realize at lower energies. As one possible example, let us envisage a UV laser. In this case, the nuclear transitions could be

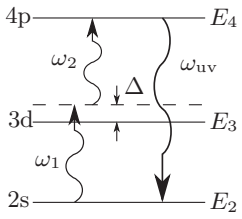

FIG. 4. Sketch (not to scale) of the level scheme. The pumping process from 2s to 4p is induced by a detuned two-photon transition, i.e., both photons together are in resonance $E_4 - E_2 = \omega_1 + \omega_2$ while one-photon absorption is suppressed by the detuning Δ where $E_3 - E_2 = \omega_1 - \Delta$. The laser operates via the one-photon transition from 4p back to 2s and emits photons of the energy $\omega_{uv} = \omega_1 + \omega_2$.

replaced by suitable electronic transitions in atoms or molecules. The pumping could be achieved either directly via a free-electron laser in the low-energy regime or indirectly via a two-photon transition generated by two optical lasers, for example.

Let us discuss the latter case using a three-level system as depicted in Fig. 4. Assuming two pump lasers with optical frequencies ω_1 and ω_2, the laser could operate in the ultraviolet regime ω_{uv}. In this case, the expression $\tilde{g} A_{pump}$ for one-photon pumping in Eq. (24) should be replaced by $\tilde{g}_{23} A_1^{pump} \tilde{g}_{34} A_2^{pump}/\Delta$. Note that the coupling constant $\tilde{g}_{23}$ of the "dipole-forbidden" 2s-3d transition is typically much smaller than $\tilde{g}_{34}$. Assuming typical values, such as a dipole coupling length of three Bohr radii, we would need pump-laser intensities of about $I_{pump} = O(10^{10}\ \mathrm{W/cm^2})$ over a length of $\mathfrak{N} = 10^4$ coherent wave trains with a detuning of $\Delta = O(10^{13}\ \mathrm{Hz})$ in order to prevent unwanted excitations of the middle 3d level. The condition for dominant coherent emission, $\tau_{sp}/\tau_{single} \ll 1$, can be fulfilled for $S_1/L_\perp^2 = O(10^5\ \mu\mathrm{m}^{-2})$, which is quite reasonable. In this scenario, the duration of the laser pulse $\tau_{st}^{(N)}$ is comparable to the length of the pump pulse $\tau_{pump} \approx \tau_{st}^{(N)} = O(10\ \mathrm{ps})$ and its intensity is well above $O(10^5\ \mathrm{W/cm^2})$, depending on the number of foils.

Again, the main idea would be that the coherent emission is strongly enhanced for $S \gg 1$ in comparison to competing noncoherent decay channels. To this end, the two pump lasers must be parallel to ensure the spatial phase matching. Let us briefly compare the envisaged (pulsed) UV laser with alternative approaches, such as (continuous) four-wave mixing, see, e.g., [46–49]. The generation of UV radiation via four-wave mixing relies on the nonlinearity of the medium, which is typically generated by an off-resonant (i.e., detuned) fourth-order quantum-mechanical scattering process. This implies that the brilliance of the outgoing beam is necessarily determined by the bandwidths of the (three) incoming laser beams. In contrast, our setup is based on resonant absorption and subsequent emission, i.e., the pumping process is temporally separated from the emission of the laser pulse. Thus, the bandwidth of the outgoing laser pulse is independent of the bandwidth of the pump pulse and solely determined by the natural or rather collective linewidth of the relevant transition.

ACKNOWLEDGMENTS

R.S. acknowledges fruitful discussions, e.g., with Bernhard Adams, at the Winter Colloquia on the Physics of Quantum Electronics (PQE), and with Uwe Bovensiepen. N.t.B. would like to thank Sumanta Das for valuable discussions at the DPG Spring Meeting in Stuttgart. This work was supported by the DFG (SFB-TR12).

APPENDIX

1. Coherent versus incoherent pumping

Let us review the pumping process by applying the Holstein-Primakoff [50] transformation

$$\hat{\Sigma}^+ = \hat{b}^\dagger \sqrt{S - \hat{b}^\dagger \hat{b}} = (\hat{\Sigma}^-)^\dagger, \quad \hat{\Sigma}^z = \hat{b}^\dagger \hat{b} - S/2, \tag{A1}$$

to the Hamiltonian in Eq. (17) and considering the limit $S \gg s$, i.e., the beginning of the pumping process

$$\hat{V}_{st} \approx \tilde{g} A_{pump}(t)(\sqrt{S}\hat{b}^\dagger + \mathrm{H.c.}). \tag{A2}$$

We first analyze the case of coherent pumping, which is pumping with a coherent pulse $A_{pump}(t)$, i.e., the same time-evolution operator applies for the whole pumping process

$$\hat{U}_{st}(t) = \exp\left(\beta(t)\hat{b}^\dagger - \mathrm{H.c.}\right). \tag{A3}$$

A time-dependent coherent state of excitons is created

$$\beta(t) = -i\tilde{g}\sqrt{S}\int_0^t d\tau\, A_{pump}(\tau), \tag{A4}$$

whose exciton number grows quadratically with time t

$$n(t) = |\beta(t)|^2 = O\left(\tilde{g}^2 S A_{pump}^2 t^2\right). \tag{A5}$$

An incoherent pump pulse, in contrast, can be approximated as a succession of many uncorrelated coherent pulses $A_{pump}^{(i)}(t)$ incident on the target. The time-evolution operator then is a product of many coherent displacement operators

$$\hat{U}_{eff} \approx \prod_i \hat{U}_{st}^{(i)} = \exp\left(\sum_i \beta_i \hat{b}^\dagger - \mathrm{H.c.}\right). \tag{A6}$$

For uncorrelated pulses, the β_i have random phases, such that the sum corresponds to a random walk

$$\beta_{eff}(j) = \sum_{i=1}^{j} \beta_i \propto \sqrt{j} \propto \sqrt{t}, \tag{A7}$$

such that the exciton number $n = |\beta_{eff}|^2$ grows merely linearly with time in this case.

2. Expressing $\tilde{g}$ in terms of Γ_{single} and ω

The coupling constant $|g_{\boldsymbol{k}}|$ can be expressed via the decay rate Γ_{single} and frequency ω

$$\Gamma_{single} = 2\pi \int d^3k\, |g_{\boldsymbol{k}}|^2 \delta(\omega_{\boldsymbol{k}} - \omega) \approx 8\pi^2 |g_{\boldsymbol{k}}|^2 \omega^2. \tag{A8}$$

The dimensionless coupling constant $\tilde{g}$ can be obtained via $\tilde{g} = |g_{\boldsymbol{k}}|\sqrt{2(2\pi)^3\omega}$ since our Hamiltonian contains the classical field $A_{pump}(t)$. As a result we arrive at

$$\tilde{g} = \sqrt{\frac{2\pi\Gamma_{single}}{\omega}}. \tag{A9}$$

[1] G. C. Baldwin and J. C. Solem, Rev. Mod. Phys. **69**, 1085 (1997).
[2] E. V. Tkalya, Phys. Rev. Lett. **106**, 162501 (2011).
[3] R. L. Mössbauer, Z. Phys. **151**, 124 (1958).
[4] R. L. Mössbauer, Naturwiss. **45**, 538 (1958).
[5] J. P. Hannon and G. T. Trammell, Hyperfine Interact. **123-124**, 127 (1999).
[6] G. V. Smirnov, U. van Bürck, W. Potzel, P. Schindelmann, S. L. Popov, E. Gerdau, Y. V. Shvyd'ko, H. D. Rüter, and O. Leupold, Phys. Rev. A **71**, 023804 (2005).
[7] D. Habs, T. Tajima, J. Schreiber, C. P. J. Barty, M. Fujiwara, and P. G. Thirolf, Eur. Phys. J. D **55**, 279 (2009).
[8] R. H. Dicke, Phys. Rev. **93**, 99 (1954).
[9] M. O. Scully, E. S. Fry, C. H. Raymond Ooi, and K. Wódkiewicz, Phys. Rev. Lett. **96**, 010501 (2006).
[10] M. O. Scully, Laser Phys. **17**, 635 (2007).
[11] E. A. Sete, A. A. Svidzinsky, H. Eleuch, Z. Yang, R. D. Nevels, and M. O. Scully, J. Mod. Opt. **57**, 1311 (2010).
[12] D. C. Burnham and R. Y. Chiao, Phys. Rev. **188**, 667 (1969).
[13] D. Fröhlich, A. Kulik, B. Uebbing, A. Mysyrowicz, V. Langer, H. Stolz, and W. von der Osten, Phys. Rev. Lett. **67**, 2343 (1991).
[14] U. van Bürck, Hyperfine Interact. **123-124**, 483 (1999).
[15] R. Röhlsberger, K. Schlage, B. Sahoo, S. Couet, and R. Rüffer, Science **328**, 1248 (2010).
[16] A. Pálffy, C. H. Keitel, and J. Evers, Phys. Rev. B **83**, 155103 (2011).
[17] R. Rohlsberger, H.-C. Wille, K. Schlage, and B. Sahoo, Nature **482**, 199 (2012).
[18] R. Schützhold, D. Habs, P. Thirolf, and M. Fujiwara, in *The White Book of ELI Nuclear Physics* (The ELI-Nuclear Physics working groups, Bucharest-Magurele, Romania), http://www.eli-np.ro/, p. 114.
[19] V. Vali and W. Vali, Proc. IEEE **51**, 182 (1963).
[20] D. Marcuse, Proc. IEEE **51**, 849 (1963).
[21] G. C. Baldwin, J. P. Neissel, L. Tonks, V. Vali, and W. Vali, Proc. IEEE **51**, 1247 (1963).
[22] V. I. Gol'danskii and Y. Kagan, Sov. Phys. JETP **37**, 49 (1973).
[23] L. Wood and G. Chapline, Nature **252**, 447 (1974).
[24] G. C. Baldwin, J. C. Solem, and V. I. Gol'danskii, Rev. Mod. Phys. **53**, 687 (1981).
[25] J. W. Eerkens, US Patent No. 3,430,046 (25 February 1969).
[26] G. C. Baldwin, Phys. Rep. **87**, 1 (1982).
[27] V. I. Vysotskii and V. I. Vorontsov, Sov. Phys. JETP **46**, 27 (1977).
[28] R. Coussement, G. Neyens, M. Van Den Bergh, and P. Boolchand, Laser Phys. **5**, 292 (1995).
[29] H. J. Lipkin, in *Multiple Facets of Quantization and Supersymmetry,* edited by M. Olshanetsky and A. Vainshtein (World Scientific, Singapore, 2002), p. 128.
[30] N. E. Rehler and J. H. Eberly, Phys. Rev. A **3**, 1735 (1971).
[31] M. O. Scully and M. S. Zubairy, *Quantum Optics* (Cambridge University Press, Cambridge, England, 1997).
[32] A. Junker, A. Pálffy, and C. H. Keitel, New J. Phys. **14**, 085025 (2012).
[33] Y. V. Shvyd'ko, T. Hertrich, U. van Bürck, E. Gerdau, O. Leupold, J. Metge, H. D. Rüter, S. Schwendy, G. V. Smirnov, W. Potzel *et al.*, Phys. Rev. Lett. **77**, 3232 (1996).
[34] R. Röhlsberger, T. S. Toellner, W. Sturhahn, K. W. Quast, E. E. Alp, A. Bernhard, E. Burkel, O. Leupold, and E. Gerdau, Phys. Rev. Lett. **84**, 1007 (2000).
[35] R. Coussement, Y. Rostovtsev, J. Odeurs, G. Neyens, H. Muramatsu, S. Gheysen, R. Callens, K. Vyvey, G. Kozyreff, P. Mandel, R. Shakhmuratov, and O. Kocharovskaya, Phys. Rev. Lett. **89**, 107601 (2002).
[36] A. Pálffy, C. H. Keitel, and J. Evers, Phys. Rev. Lett. **103**, 017401 (2009).
[37] B. W. Adams, J. Mod. Opt. **58**, 1638 (2011).
[38] K.-J. Kim, Y. Shvyd'ko, and S. Reiche, Phys. Rev. Lett. **100**, 244802 (2008).
[39] T. J. Bürvenich, J. Evers, and C. H. Keitel, Phys. Rev. Lett. **96**, 142501 (2006).
[40] A. Pálffy, J. Evers, and C. H. Keitel, Phys. Rev. C **77**, 044602 (2008).
[41] W.-T. Liao, A. Pálffy, and C. H. Keitel, Phys. Lett. B **705**, 134 (2011).
[42] http://hasylab.desy.de/e70/e6129/e4242/e4370/felbasics_eng.pdf.
[43] U. van Bürck, D. P. Siddons, J. B. Hastings, U. Bergmann, and R. Hollatz, Phys. Rev. B **46**, 6207 (1992).
[44] G. Geloni, V. Kocharyan, and E. Saldin, DESY **11–224** (2011).
[45] B. J. Siwick, J. R. Dwyer, R. E. Jordan, and R. J. D. Miller, Science **302**, 1382 (2003).
[46] K. S. E. Eikema, J. Walz, and T. W. Hänsch, Phys. Rev. Lett. **83**, 3828 (1999).
[47] K. S. E. Eikema, J. Walz, and T. W. Hänsch, Phys. Rev. Lett. **86**, 5679 (2001).
[48] M. Scheid, D. Kolbe, F. Markert, T. W. Hänsch, and J. Walz, Opt. Express **17**, 11274 (2009).
[49] D. Kolbe, A. Beczkowiak, T. Diehl, A. Koglbauer, M. Sattler, M. Stappel, R. Steinborn, and J. Walz, Hyperfine Interact. **212**, 213 (2012).
[50] T. Holstein and H. Primakoff, Phys. Rev. **58**, 1098 (1940).